550 kV HVDC Transmission Line Surge Arrester: EMTP-ATP Simulation Model

Cristian C. Acosta C.
Universidad Nacional de Colombia
EMC-UN Group – Universidad Nacional de Colombia
Bogotá D.C., Colombia
ccacostac@unal.edu.co

Francisco Román
Universidad Nacional de Colombia
EMC-UN Group – Universidad Nacional de Colombia
Bogotá D.C., Colombia
fjromanc@unal.edu.co

***Abstract*— An EMTP-ATP simulation model of a 550 kV HVDC transmission Line Surge Arrester (LSA) is presented. In addition to the LSA models, the tower, insulators, conductors, grounding resistance are also included in the simulation. The EMTP-ATP simulations models are used to calculate the expected overvoltages caused by direct impact to the power conductor and direct impact to the tower (tower strike).**

Keywords*— *LSA, HVDC, direct impact to the power conductor, tower strike, critical flashover voltage, Line Surge Arrester, transient overvoltage

I. INTRODUCTION

The Colombian Mining/Energy Planning Unit (UPME Spanish acronym for Unidad de Planeación Minero-Energética) -UPME- is projecting the installation of two HVDC (High Voltage Direct Current) transmission projects in the Colombian territory: the first one is a ±450 kV HVDC to connect Panamá; and the second one is a ±550 kV to connect the Cerromatoso nickel mining company [2][3]. However, both projects are in areas with very high lightning flash densities -GFD-. Therefore, the aim of the present work is to determine the HVDC transmission line arresters protection level in the case of direct impact to a power conductor and a tower strike.

II. SIMULATION MODELS

A. Transmission tower simulation model

To perform the analysis of the transient behavior produced by the lightning impact on an HVDC line, it is necessary to model the transmission line by means of an equivalent circuit with passive elements (impedances) that simulates the behavior of the traveling wave in the tower structure, insulators string (to check the existence of flashover or back flashover) and grounding resistance. Fig. 1 shows the transmission tower model of a compact HVDC line at ±500 kV (at present there are no projects at ±550 kV) and its equivalent circuit. The objective of compacting a transmission line is to reduce costs in material and land acquisition for Right-Of-Way, maintaining the same distances of security and isolation as in a conventional HVDC line [4].

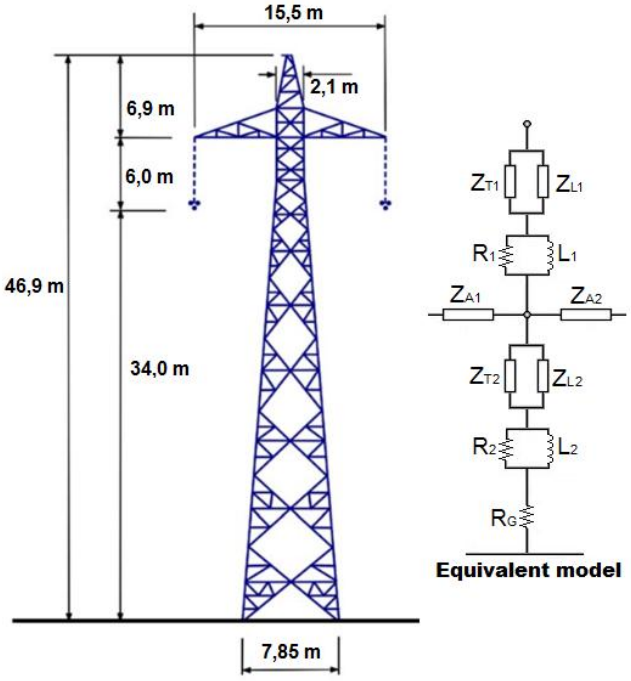

Figure 1. HVDC transmission tower and equivalent circuit

To implement the transmission tower model, its topology and geometry must be considered, for which the model suggested by Kim et al. [5] is used, which includes the effect that transient overvoltage has on the tower body (Multi-Story transmission line model [6][7]), the tower arms and the effect on the tower body (Hara model [8]), and the wave attenuation when passing through each section of the tower (Ishii model [6][7]).

In the following is presented the methodology to obtain the equivalent parameters of the tower model.

1) Surge impedance (Z_T):

The corrected CIGRE formula is used due to the proximity of the results obtained with the formula with respect to the experimental measurements [5].

$$Z_T = \sqrt{\frac{\pi}{4}} \cdot 60 \cdot \left(ln\left(cot\left(\frac{1}{2} \cdot arctan\left(\frac{R_{avg}}{H} \right) \right) \right) - ln\sqrt{2} \right) \quad (1)$$

Where: H is tower height and R_{avg} is average radius. The surge impedance Z_T for this case is **179.34 Ω.**

2) Parallel surge impedance (Z_L) and crossarm surge impedance (Z_A):

The parallel surge impedance Z_L represents a reduction of 90% of surge impedance Z_T when bracings are added to tower base, the value of Z_L is determined:

$$Z_L = 9 \cdot Z_T \tag{2}$$

In this case, Z_L is **1614.07 Ω**. The crossarm surge impedance Z_A formula is:

$$Z_A = 60 \cdot ln\left(\frac{2 \cdot h_A}{r_A}\right) ; \; r_A = \frac{l_A}{4} \tag{3}$$

Where: h_A and r_A are the height and equivalent radius of crossarm tower (a quarter of crossarm length). In this case, Z_L is **223.24 Ω**.

3) R-L parallel circuit in series with Z_T:

The traveling wave experiences an attenuation through the tower that is represented by a RL parallel circuit connected in series with surge impedances Z_T (see Eq. 1). The values of R and L are determined with formulas:

$$R_i = \frac{-2 \cdot Z_T \cdot ln\sqrt{\gamma}}{H} \cdot h_i \tag{4}$$

$$L_i = \alpha \cdot R_i \cdot \frac{2H}{c} \tag{5}$$

Where: Z_T is the surge impedance, H is the tower height, h_i is the i^{th} section length, γ is attenuation coefficient (between 0.7 and 0.8), α is damping coefficient (usually it is 1) and c is speed of light (3.10^8 m/s). Applying the formulas result the following values:

R_1: **5.89 Ω**; L_1: **1.84 µH**; R_2: **34.31 Ω**; L_2: **10.67 µH**.

Finally, the equivalent circuit transmission tower shown in Figure 2 is obtained in EMTP-ATP. The other elements of the circuit model are obtained as it is explained in the following paragraphs:

4) Grounding resistance model (R_G):

The grounding resistance is dependent on the current flowing through it. The following expression is used:

$$R(I) = \frac{R_0}{\sqrt{1 + I/I_g}} \; ; \left(I_g = \frac{E_0 \rho}{2\pi {R_0}^2}\right) \tag{6}$$

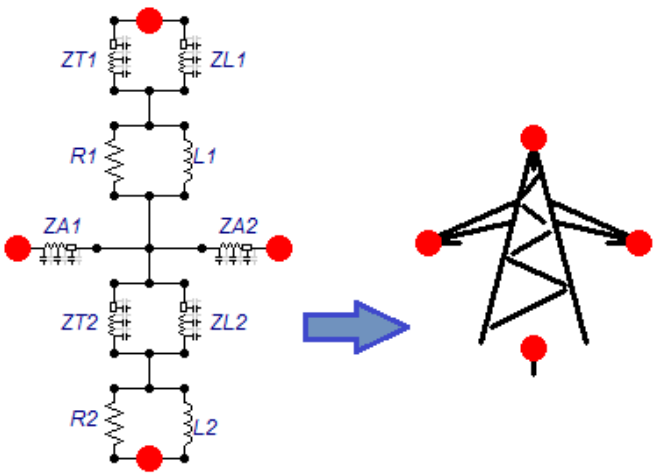

Figure 2. Equivalent circuit of transmission tower

Where: *R(I)* is the grounding resistance, R_0 is the footing resistance at low current and low frequency (10 Ω), I is strike current, I_g is limiting current of soil ionization, ρ is the soil resistivity (100 Ω.m) and E_0 is the soil ionization gradient (300 kV/m). A "*Model*" was used in ATP to simulate the non-linear behavior of the grounding resistance.

5) Insulator string model:

The insulator string model consists of a capacitor connected in parallel to a voltage-controlled switch, where the capacitor represents the capacitance of the insulator string and the voltage-controlled switch represents the flashover before an impulse voltage that exceeds the dielectric strength of the insulator. TABLE 1 shows the main parameters of a ±500 kV insulator string.

Fig. 3 based on Eq. 18 of the standard IEEE 1243-1997 [9][10], shows the V-t characteristic of the insulator string before a transient overvoltage. The insulator string model is connected between positive pole and tower structure.

TABLE 1. MAIN PARAMETERS OF A ±500 KV INSULATOR STRING [4]

Number of discs	**25**
Diameter	**380 mm**
Weight/disc	**15.4 kg**
String length	**5 m**

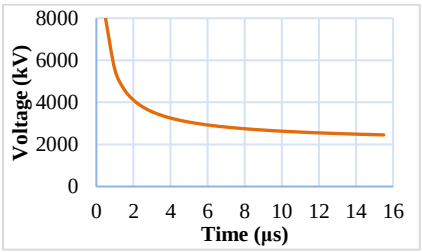

Figure 3. V-t insulator characteristic based on the standard IEEE 1243-1997

B. *Line Surge Arrester simulation model*

The Line Surge Arrester simulator model is composed of two parts: the surge arrester (Series Varistor Unit), and the series air gap. Each part is modeled separately in EMTP-ATP and then connected in parallel to the insulator of the line.

1) Surge arrester simulation model

The IEEE proposes a frequency-dependent model for the surge arrester [11]. The surge arrester model is presented in Figure 4.

Where: L0 represents the magnetic fields near the surge arrester, R0 is used to provide stability to the simulation results, C is the capacitance between the terminals of the surge arrester, L1 and R1 form a low-pass filter, and the non-linear resistances A0 and A1 represent the non-linear characteristic of the surge arrester [12]. Each of these parameters is determined with the following equations:

$$\begin{aligned} L0 &= 0.2 \cdot d/n\ [\mu H] \\ R0 &= 100 \cdot d/n\ [\Omega] \\ L1 &= 15 \cdot d/n\ [\mu H] \\ R1 &= 65 \cdot d/n\ [\Omega] \\ C &= 100 \cdot n/d\ [C] \end{aligned} \tag{7}$$

Where: *d* and *n* are the length and number of arrester columns. For the present case of study, the number of varistors is **3** and the length of the surge arrester is **3.6 m**. To determine the values of A0 and A1 the modified values are presented in TABLE 2 applying the Eq. 8.

$$A_{0,1} = \left(Relative\ IR\ for\ A_{0,1}(i)\right) \cdot V_{10}/1.6 \tag{8}$$

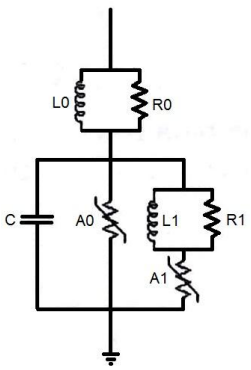

Figure 4. The IEEE surge arrester model

Where V_{10} is the discharge voltage in kV for a 10 kA, 8/20μs current [10]. According to characteristic VI for the ±500 kV line surge arrester [12] V_{10} is 931 kV, however, as the HVDC line in this article has a higher 50 kV voltage, V_{10} is increased by the same magnitude, so that the value used for the expressions in Eq. 8 is 981 kV.

TABLE 2. V-I CHARACTERISTICS FOR A0 AND A1

Current	Voltage for A0 (p.u)	Voltage for A1 (p.u)
10 μA	0.85	0.6
100 μA	1.05	0.84
1 mA	1.19	0.94
10 mA	1.23	0.97
100 mA	1.28	1
1 A	1.33	1.04
10 A	1.4	1.1
100 A	1.54	1.23
1 kA	1.68	1.36
2 kA	1.73	1.41
4 kA	1.78	1.47
6 kA	1.82	1.51
8 kA	1.86	1.54
10 kA	1.9	1.56
12 kA	1.93	1.58
14 kA	1.97	1.6
16 kA	2	1.62
18 kA	2.05	1.64
20 kA	2.1	1.66
50 kA	2.4	1.82
100 kA	2.68	1.95
200 kA	2.96	2.1
300 kA	3.23	2.23

In general, the values of A0 and A1 are well adjusted to the measurements made by the manufacturers of the surge arresters, however, it is necessary to include the voltage and current values of the Maximum Continuous Operating Voltage - MCOV- [13]. The MCOV information is important because it is essential to guarantee the extinction of the follow current in the series air gap after the lightning strike, and the HVDC transmission line continues with its normal operation. The cells shaded in blue in the TABLE 2 indicate the values added to characteristic V-I of A0 and A1.

2) Series air gap simulation model

A model representing the dynamic behavior of air resistance based on equations of experimental measurements made by several researchers [15][16] is used. The air gap is represented by the equivalent circuit shown in Figure 5. Where: R_{fuga} is the leakage resistance, *C* is the own capacitance, *SVC* is the voltage-controlled switch that represents the activation of the air gap, R_{gap} is the air gap electrical resistance during its activation gap. Both R_{fuga} and *C* have set values of 10^{24} Ω and 10^{-24} F, respectively [12]). For *SCV* and R_g, additional considerations must be taken because *ATP-Models* are used for their modeling.

a) Voltage-controlled switch for air gap simulation model: This *ATP-Model* represents the activation of the air gap when the Critical Flashover Voltage is reached, this voltage is defined by the V-t characteristic presented in [17], which is compared with the V-t insulator characteristic (Figure 3) to analyze the insulation coordination in the system.

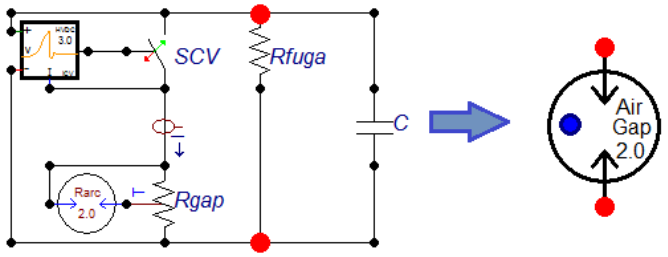

Figure 5. Equivalent circuit and air gap icon

Figure 6 shows the comparison of both air gap (blue) and insulator (orange) V-t characteristics. It is evident that in the event of an overvoltage incident in the elements, the critical flare voltage is reached first in the air gap, complying with the insulation coordination and the protection of the insulator. As explained in [18][19] for a ±500 kV line, a BIL of 1150 kV is set.

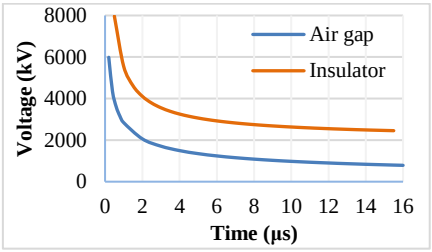

Figure 6 V-t characteristic of air gap (blue) and insulator (orange)

b) Series air gap simulation model: As presented in [12][15][16], it is observed that the Barannik resistance model is the most optimal to represent the dynamic behavior of the resistance, due to the variables it takes into account and the simplicity of implement the *ATP-Model*. The expression to determine the Barannik resistance is presented in Eq. 9.

$$R(i) = \frac{C \cdot d \cdot {\rho_0}^{1/3}}{\int_0^{\tau} i^{2/3} \cdot dt} \qquad (9)$$

Where: *R(i)* is the air electric resistance gap depending on the current, *C* is the model constant ($0.7*10^{-3}$ to $1.7*10^{-3}$), *d* is the gap length and ρ_0 is the air density.

III. SIMULATION RESULTS

It is expected that the LSA protects the insulator string against direct impact to a power conductor and/or tower strike caused overvoltages. The simulations are performed by applying to the model alternatively 10/350µs for direct impact to a power conductor or tower strike lightning current impulses of different amplitudes. For tower strike it starts with 20 kA and variations are made every 20 kA up to 100 kA, from 100 kA variations are made every 50 kA up to 300 kA; for direct impact to a power conductor it starts with 10 kA and variations are made every 10 kA up to 50 kA assuming there is a shield failure. Simulations are only made with the LSA connected to the positive pole, so most of the lightning strike to ground are negative [20].

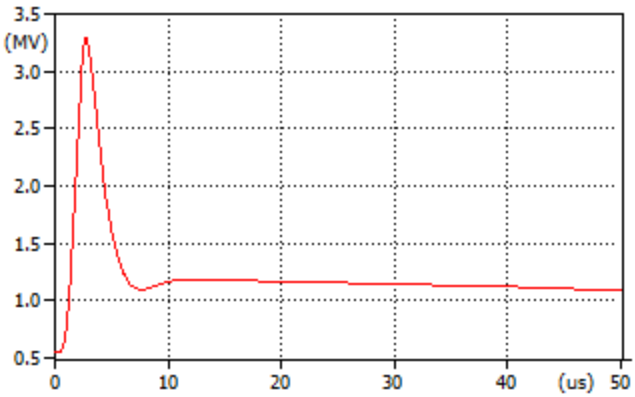

Figure 7 Insulator voltage waveform without LSA for tower strike (Lightning current = 250 kA)

In the present numerical simulation and for tower strike, the lightning current amplitude was varied from 20 kA to 300 kA as it is recommended in [4]. However, back flashover was reached in the positive insulator when the lightning current is 300 kA in an insulator that has no connected an LSA. The insulator voltage waveform for a lightning current of 250 kA is shown in Figure 7, the overvoltage peak reached is 3,29 MV.

For a lightning current from 10 to 300 kA which impacts a tower with LSA the overvoltage is reduced in all cases. The LSA current and voltage waveform is shown in Fig. 8 and Fig. 9, respectively.

Following, the comparative charts for voltage in positive pole, voltage in negative pole, current in the LSA and energy in the LSA for all cases are presented. For the direct impact to a power conductor analysis, are only shown the cases with an LSA connected. The reason is that the CFO of the insulator string is reached for a current lower than those mentioned in the simulation methodology for the case when the LSA is not present.

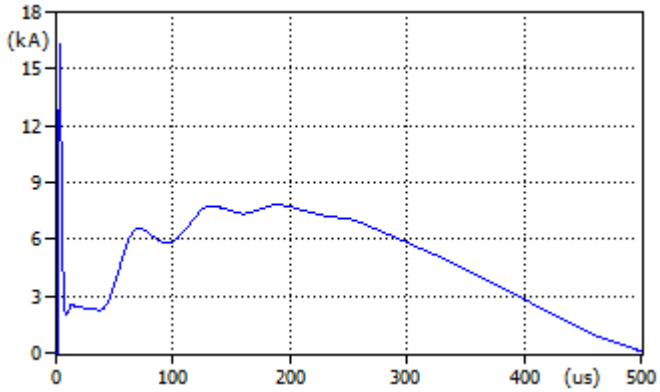

Figure 8 LSA current waveform for tower strike (Lightning current = 300 kA)

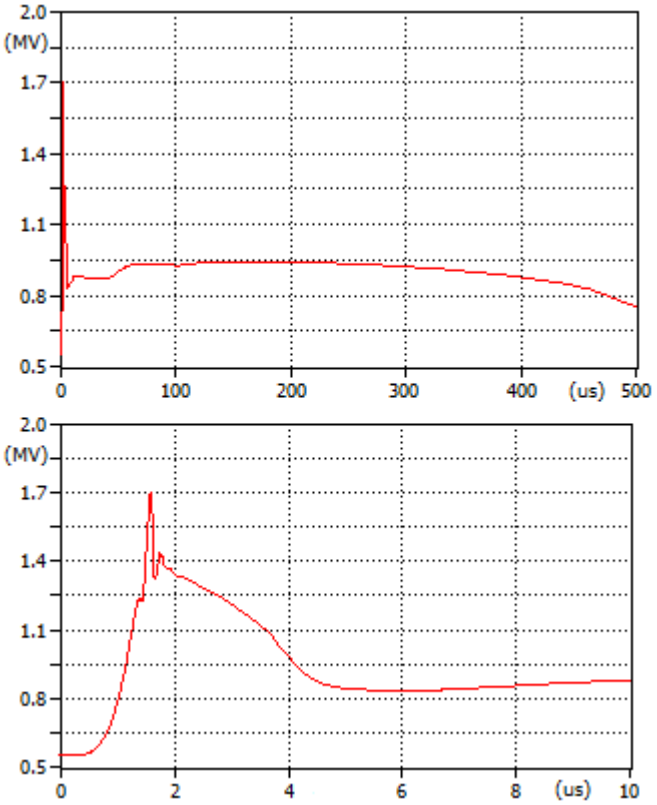

Figure 9 LSA voltage waveform for tower strike with different time scale (Lightning current = 300 kA)

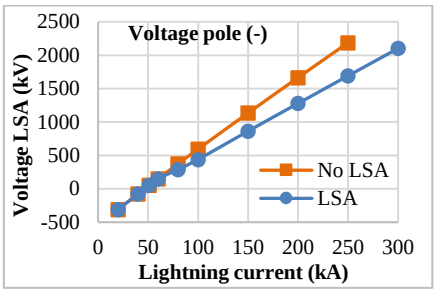

Figure 10. Voltage in negative pole for tower strike

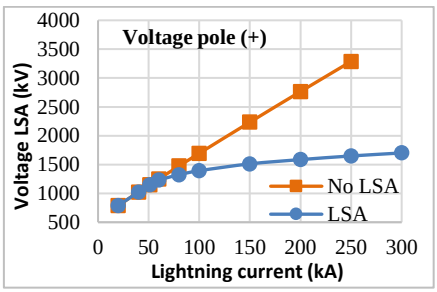

Figure 11. Voltage in positive pole for tower strike

The curves in Fig. 10 and Fig. 11 reach up to 250 kA when the LSA is not connected. This result shows the importance of the use of LSA to reduce the adverse effect that a possible tower strike can cause on the transmission line operation.

For both the positive pole and the negative pole, it is possible to verify the LSA operation in HVDC transmission lines, mainly because it reduces the voltage that reaches the insulator in each pole. The voltage reduction is more important at the positive pole, mainly because the LSA is connected there. The lightning current that activates the LSA is 51.14 kA. Therefore, for smaller currents the LSA does not suppress the overvoltage in the insulator.

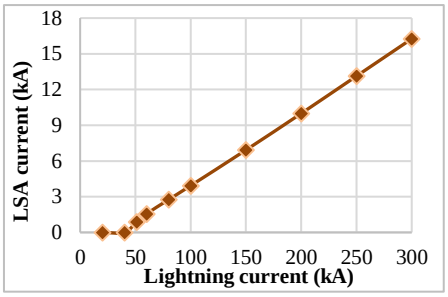

Figure 12. LSA current for tower strike

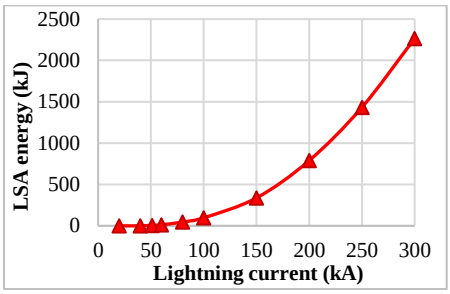

Figure 13. LSA energy for tower strike

As it can be seen in Fig. 12 and Fig. 13, when the lightning current increases, the current and energy in the LSA show a respective linear and polynomial increase ($E \approx I^2$). The most remarkable result in that the maximum energy that reaches the LSA at the maximum impact current (300 kA) is 2265.5 kJ. In [13] is mentioned that the maximum energy absorbed by the LSA for a current of 400 kA is 1200 kJ, therefore it is possible that the large difference of energy values is due to the waveform used in [13], the nominal values of the LSA for a 8/20µs waveform, and finally, due to the fact that the present simulation was made with a 10/350µs waveform (wave with higher energy content).

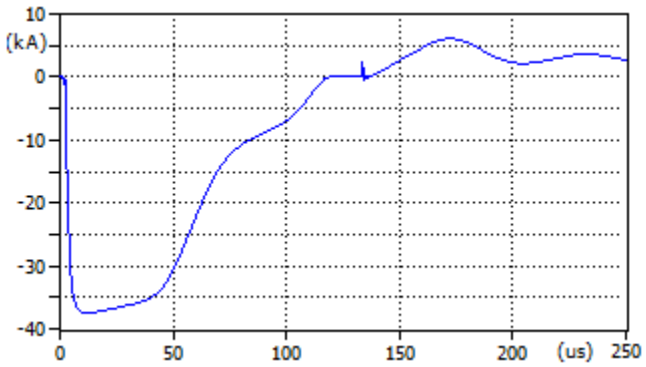

Figure 14 LSA current waveform for direct impact to a power conductor (Lightning current = 50 kA)

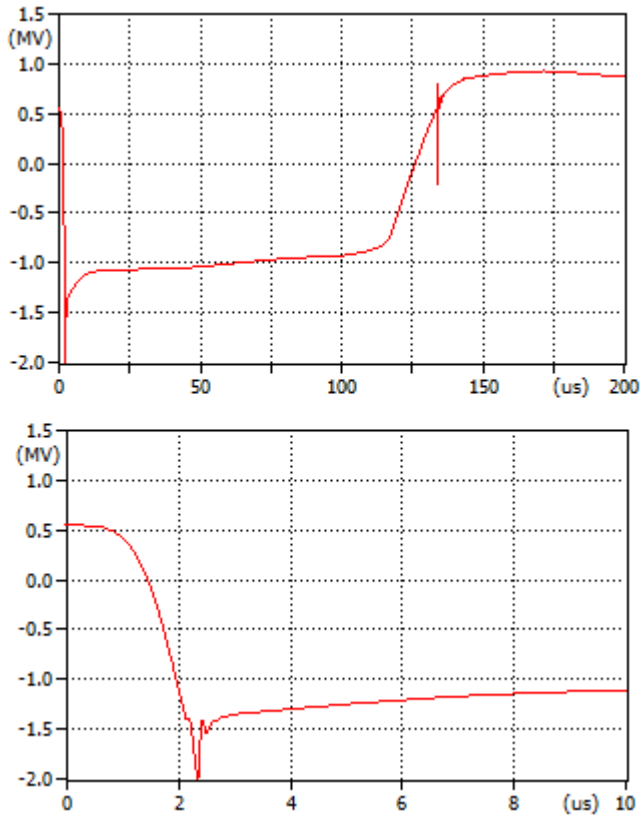

Figure 15 LSA voltage waveform for direct impact to a power conductor with different time scale (Lightning current = 50 kA)

The LSA current and voltage for direct impact to a power conductor case is shown in Fig. 14 and 15, respectively. The overvoltage peak is -2 MV and the maximum current in LSA is -37,5 kA. When the line voltage attempts to stabilize its value at 550 kV, a second activation of the LSA occurs. This is because the voltage in the air gap reaches its activation value again, after this, the voltage line transient is extinguished until it reaches its stable value.

In the charts presented in Fig. 16 to 19, there is not a direct proportional relationship between the increase in the lightning current and the increase in overvoltages, mainly because in all direct lightning strike cases, the LSA is activated. However, the most noticeable result is that in any circumstance, the Critical Flashover Voltage of the insulator string is reached. Therefore, under these conditions, the normal operation of the line can be guaranteed with the use of the LSA.

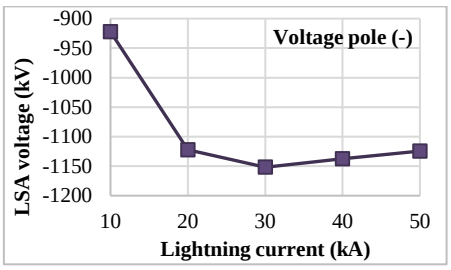

Figure 16. Voltage in negative pole for direct impact to a power conductor

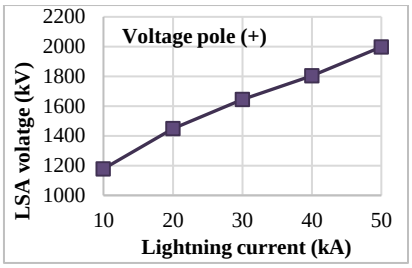

Figure 17. Voltage in positive pole for direct impact to a power conductor

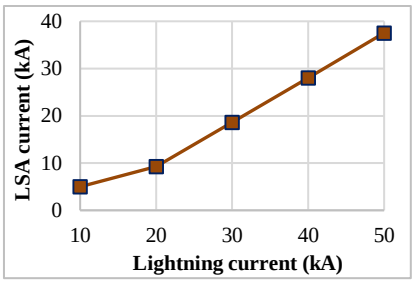

Figure 18. LSA current for direct impact to a power conductor

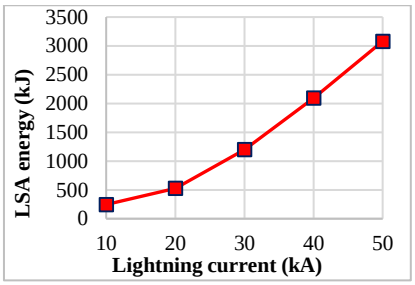

Figure 19. LSA energy for direct impact to a power conductor

The results of current and energy in an LSA for direct impact to a power conductor are like those obtained for tower strike. However, the magnitudes are much higher, this is because in the case of tower strike portion of lightning current goes through of grounding resistance, which plays an important role in the protection of the HVDC transmission lines.

IV. CONCLUSIONS

It is possible to determine the protection level provided by the line arresters in the HVDC transmission towers, showing favorable results in all cases in which the lightning strikes a tower with an installed Line Surge Arrester.

Despite not finding an existing configuration of an HVDC line of ±550 kV, the results obtained with a HVDC line of ±500 kV are valid for the theoretical analysis carried out. The safety distances and the geometry of the towers are close, as are the length of the insulators and the of the grounding resistance.

Variations in the lightning waveform affect the surges produced on the line insulators. From this result, it is also possible to determine that an LSA at the positive isolator also reduces the overvoltage produced in the negative isolator of the same impacted tower.

REFERENCES

[1] C. Acosta. Estudio mediante modelos de simulación de descargadores de línea en torres de transmisión HVDC en la zona intertropical de Sudamérica. Master's thesis, Universidad Nacional de Colombia, 2019.

[2] UPME-Unidad de Planeación Minero Energética. Plan de expansión de referencia generación-transmisión 2016-2030, 2017.

[3] UPME-Unidad de Planeación Minero Energética. Plan de expansión de referencia generación-transmisión 2017-2031, 2018.

[4] M. Salimi. *A new approach for compaction of HVDC transmission lines and the assessment of the electrical aspects*. PhD thesis, University of Manitoba, 2017.

[5] J. Kim, L. Czumbil, and H. Nouri. *Component model e_ect on fastfront overvoltages in Gas Insulated Substations*. In 2015 50th International Universities Power Engineering Conference (UPEC), pages 1-6. IEEE, 2015.

[6] Juan A Martinez-Velasco. *Power system transients: parameter determination*. CRC press, 2017.

[7] M. Ishii, T. Kawamura, T. Kouno, E. Ohsaki, K. Shiokawa, K. Murotani, and T. Higuchi. *Multistory transmission tower model for lightning surge analysis*. IEEE Transactions on Power Delivery, 6(3):1327-1335, July 1991.

[8] T. Hara and O. Yamamoto. *Modelling of a transmission tower for lightning-surge analysis*. IEEE Proceedings - Generation, Transmission and Distribution, 143(3):283-289, May 1996.

[9] IEEE. *IEEE 1243-1997 Guide for Improving the Lightning Performance of Transmission Lines*, Dec 1997.

[10] X. Wang, Z. Yu, and J. He. *Breakdown Process Experiments of 110- to 500-kV Insulator Strings Under Short Tail Lightning Impulse.* IEEE Transactions on Power Delivery, 29(5):2394-2401, Oct 2014.

[11] IEEE Transactions on Power Delivery, *Modeling of metal oxide surge arresters,* 7(1):302-309, Jan 1992.

[12] C. Landinez, C. Gómez, J. Arias, H. López, F. Román. *Modelamiento de protecciones utilizando ATP*. Universidad Nacional de Colombia, 2008.

[13] S. Gu, S. Wan, J. Wang, J. Chen, and T. Li. Development and Application of ±500 kV DC Transmission Line Arrester in China Power Grid. IEEE Transactions on Power Delivery, 33(1):209-217, Feb 2018.

[14] J. Rodríguez. Estudio del envejecimiento de descargadores de sobretensión en la región de máxima tensión de operación continua empleando una fuente de corriente de extra alta impedancia. Master's thesis, Universidad Nacional de Colombia, 2017.

[15] R. Montaño, M. Becerra, V. Cooray, M. Rahman, and P. Liyanage. *Resistance of spark channels*. IEEE Transactions on Plasma Science, 34(5):1610-1619, Oct 2006.

[16] Ji-ling, Z. and Hua-mao, Z. and Cheng-nan, Z. and Shao-feng, D. *Spark model for 1100kv gis disconnecting switch*. In 2011 1st International Conference on Electric Power Equipment - Switching Technology, pages 504-508, Oct 2011.

[17] Hao, Yanpeng and Han, Yongxia and Tang, Li and Mao, Changgeng and Li, Licheng. *Leader propagation models of ultrahigh-voltage insulator strings based on voltage/time curves under negative lightning impulses at high altitude.* IEEE Transactions on Dielectrics and Electrical Insulation, 22(2):1186-1192, 2015.

[18] S. Furukawa, O. Usuda, T. Isozaki, and T. Irie. *Development and applications of lightning arresters for transmission lines.* IEEE Transactions on Power Delivery, 4(4):2121-2129, Oct 1989.

[19] K. Ishida, K. Dokai, T. Tsozaki, T. Irie, T. Nakayama, H. Fujita, K. Arakawa, and Y. Aihara. *Development of a 500 kv transmission line arrester and its characteristics.* IEEE Transactions on Power Delivery, 7(3):1265-1274, July 1992.

[20] R. Cuarán. Análisis de apantallamiento en líneas de extra y ultra alta tensión mediante el Modelo Auto-Consistente de Interceptación de Rayos-SLIM. Master's thesis,Universidad Nacional de Colombia, 2015.